Science Journal of University of Zakho
DOI: https://doi.org/10.25271/sjuoz

Original article

# SOLVOTHERMAL SYNTHESIS OF HIGHLY LUMINESCENT GRAPHENE QUANTUM DOTS FROM GRAPHENE OXIDE FOR DUAL APPLICATIONS IN COPPER ION SENSING AND NANOTHERMOMETRY

**Sitya Hishyar Ali[1*] and Diyar Sadiq[2]**

[1] Department of Physics, College of Science, University of Zakho, Zakho, Kurdistan Region, Iraq.
[2] Directorate of the Scientific Research Center, Duhok Polytechnic University, Duhok, 61 Zakho Road, Kurdistan Region, Iraq.
[*] Corresponding author. E-mail: sitye.ali@staff.uoz.edu.krd (Tel: +964-7507885624)

Received: 29, Jun, 2025
Accepted: 17, Aug, 2025
Published: 18, Jan, 2026

**ABSTRACT**

This research effectively produced graphene quantum dots (GQDs) utilizing a solvothermal method from graphene oxide (GO) with N, N-dimethylformamide (DMF) as the solvent. Transmission Electron Microscopy (TEM) analyses revealed that the produced GQDs primarily exhibited a spherical morphology, with uniformly distributed nanoparticles and a mean diameter of 4.12 nm. Photoluminescence (PL) studies show excitation-dependent green emission characteristics, with an emission wavelength of 551 nm under 500 nm excitation. This is associated with a high PL intensity and a quantum yield (QY) of 51.56%. X-ray diffraction (XRD) results confirmed that the GQDs have a graphitic structure. Fourier Transform Infrared Spectroscopy (FTIR) and Energy-Dispersive X-ray spectroscopy (EDX) confirmed the presence of oxygen functional groups, with carbon, oxygen, and nitrogen as the primary elemental components, verifying the nitrogen doping of the GQDs. The absence of other metals shows that the synthesized GQDs have a high level of purity. The synthesized GQDs were successfully utilized as an ion sensor for detecting Cu2+ ions, highlighting their exceptional sensitivity and selectivity with a limit of detection of 0.55 µm. The GQDs also exhibit potential nanothermometric behavior, as they display a photoluminescence response that depends on temperature with a sensitivity of 1.81% °C-1 between 20 °C and 70 °C. By combining nitrogen doping with a simple solvothermal synthesis, this research produces dual-function GQDs that enable both highly sensitive detection of Cu2+ ions and reliable temperature sensing.

**KEYWORDS:** Graphene quantum dots (GQDs), Cu2+ sensor, Nanothermometer, Fluorescence, Solvothermal.

## 1. INTRODUCTION

Graphene consists of a single layer of carbon atoms arranged in a honeycomb structure, identified in 2004 through $sp^2$ hybridization (Novoselov *et al.*, 2004). This complex material is essentially a single layer of graphite, exhibits exceptional mechanical durability, high thermal conductivity, a significant specific surface area, enhanced carrier mobility, and chemical reactivity at ambient temperatures (Krishnan *et al.*, 2019; Li *et al.*, 2015). The properties of graphene enable its utilization in several applications, including sensors (Tanguy *et al.*, 2019), energy storage devices (Allahbakhsh & Arjmand, 2019), solar cells, and medicine delivery (Yang *et al.*, 2016). Graphene is classified as a zero-bandgap semiconductor, meaning it does not exhibit optical photoluminescence (PL) in its pure form. These characteristic limits its use in optoelectronic applications. Dividing graphene into nanometer-scale fragments, known as graphene quantum dots (GQDs), is an effective strategy for addressing this challenge (Pan *et al.*, 2010b; Zhang *et al.*, 2008). GQDs are zero-dimensional materials derived from graphene and carbon dots (CDs), which are considered small graphene fragments (Shen *et al.*, 2012; Shi *et al.*, 2023). Graphene quantum dots inherit graphene's properties of graphene and exhibit a range of unique behaviors under diverse physical and chemical conditions (Rajender *et al.*, 2017). In comparison to graphene, GQDs demonstrate strong quantum limitations and boundary effects(Fan *et al.*, 2023), *which* provide several advantages, including stable fluorescence characteristics that can be modified through doping or by controlling their size and morphology (Kharangarh, Ravindra, *et al.*, 2023), photoluminescence (PL) is a notable characteristic of GQDs, since emit a spectrum of photoluminescent colors depending on the synthesizing techniques applied(Fan *et al.*, 2015), minimal cellular toxicity(Reghunath *et al.*, 2023; Zhang *et al.*, 2022), and ideal water dissolvability(Hsieh *et al.*, 2023; Zeng *et al.*, 2022). Consequently, GQDs have an expanded range of applications across various fields, including optoelectronic devices (Kurniawan *et al.*, 2021), sensors (Kharangarh, Singh, *et al.*, 2023; Yu *et al.*, 2025), bioimaging(Bayat & Saievar-Iranizad, 2017; Yan *et al.*, 2018), drug delivery(Jiang *et al.*, 2015), energy(Su *et al.*, 2020), and environment monitoring(Jin *et al.*,

Access this article online
https://doi.org/10.25271/sjuoz.2026.14.1.1654
Printed ISSN 2663-628X;
Electronic ISSN 2663-6298
Science Journal of University of Zakho
Vol. 14, No. 01, pp. 151 –161 January-2026

2015). GQDs can be produced with two principal methodologies: top-down and bottom-up. The top-down process starts with substantial carbon-derived resources, such as graphite and GO, as starting materials. These materials are then broken down into the required GQDs through several chemical, thermal, or physical treatments. Oxidative or reductive cleavage, electrochemical fragmentation, and pulsed laser ablation (PLA) are techniques employed in the top-down synthesis approach (Shin *et al.*, 2015). The bottom-up technique involves integrating small starting compounds, such as citric acid and aromatic compounds, into larger frameworks to produce GQDs. The principal synthesis methods include hydrothermal/solvothermal, microwave-assisted, soft-template, and progressive organic production processes(Allahbakhsh & Bahramian, 2018). The methods outlined facilitate precise control of GQD dimensions; however, they often require selecting specific organic materials as precursors and involve complex reaction procedures. The solvothermal reaction is a synthetic process that falls into two primary categories: it uses organic solvents such as benzene, DMF, DMSO, CH3OH, DCM, concentrated H2SO4, and HNO3 to convert GO into GQDs, rather than water, to obtain the desired reaction products. Organic solvents significantly affect the dimensions and shapes of the products; thus, it is essential to investigate their chemical nature and physicochemical properties (Zhu *et al.*, 2011). The solvothermal method presents numerous advantages. It is economical, cost-effective, and non-toxic(Kharangarh, Ravindra, *et al.*, 2023). Previous studies have focused on using GO as a starting material for the synthesis of GQDs via solvothermal methods. These studies used various solvents to evaluate their effects on the sizes, yields, and optical properties of the resulting GQDs. For instance, Jiang, Dan, et al. *(*Jiang *et al.*, 2015) effectively synthesized GQDs from GO using a solution of $H_2O_2$ and iron(III) chloride ($FeCl_3$), achieving a remarkable quantum yield of 24.6%. These GQDs exhibit intense PL, indicating good biocompatibility. Su, Jie, et al. (Su *et al.*, 2020) effectively synthesized N-GQDs from GO using ethylenediamine (EDA), $H_2O_2$, and ultra-pure water. The quantum yield of these N-GQDs attained roughly 46%. The findings suggest that these N-GQDs could penetrate tissues through endocytosis, indicating their potential as fluorescent probes for biological imaging. Zhu and colleagues (Zhu et al., 2011) produced brightly green-emitting GQDs from GO via a solvothermal approach. These GQDs exhibit quantum yields beyond 11.4%. Dimethylformamide (DMF) plays a crucial role in the solvothermal preparation of GQDs, significantly influencing the frameworks and optical properties of these nanomaterials. In the high-temperature heating process, DMF served as both a nitrogen source and solvent, allowing nitrogen to be doped into the graphene lattice in situ. The doping of nitrogen atoms creates surface defect states, thereby altering the electronic structure of the GQDs and improving PL intensity and QY (Carrera *et al.*, 2025; Martins *et al.*, 2025). It has been demonstrated that the selection of a solvent (DMF) in this case impacts the order of the edge states and functional groups found on the surfaces of GQDs, which in turn influences the emission and quantum efficiency. Additionally, DMF has been shown to enhance control over the dimensions and surface chemistry of GQDs, which are crucial for tuning their optical properties. Although significant advancements have been made in synthesizing GQDs, achieving both high quantum yield (QY) and dual applications remains challenging. Several studies that utilize DMF as a solvent have reported moderate optical performance, often due to suboptimal reaction conditions or insufficient control over surface functionalities. Furthermore, existing literature seldom showcases GQDs that achieve both high QY and dual functionality, such as simultaneous ion sensing and nanothermometry (Lin & Zhang, 2012; Pan et al., 2010a; Shin et al., 2014; Zhu et al., 2011).Graphene quantum dots (GQDs) were produced in this study through a solvothermal process, with graphene oxide (GO) serving as the starting material and DMF as the solvent. This method endowed these GQDs with a significantly high PL intensity and quantum yield, superior to most as-prepared GQDs. The GQDs display excitation-dependent green photoluminescence, and a range of characterizations was carried out to study their shape, arrangement, composition, and optical characteristics. Such remarkable optical properties rendered them practical for application as a fluorescence indicator for $Cu^{2+}$ ions, with a low limit of detection of 0.55 μM, and as a prospective nanothermometer, demonstrating a temperature sensitivity of 1.81% $°C^{-1}$ in the physiological temperature range. This study indicates that DMF, as the solvent, exhibits the highest enhancement effect on the optical characteristics of GQDs, which may enable unique sensing and thermoresponsive applications of GQDs. This offers essential concepts for solvent-mediated GQD synthesis regarding potential nanomaterial applications.

## 2. MATERIALS AND METHODS

### Materials and Reagents:

Graphite powder (99.5%) was acquired from CDH, India. Potassium permanganate ($KMnO_4$, 99-100.5 %), Sodium nitrate ($NaNO_3$, 99%), Sulfuric acid ($H_2SO_4$, 98%), Hydrogen peroxide ($H_2O_2$, 30%), Hydrochloric acid (HCl, 37%), N, N-dimethylformamide (DMF) were all purchased from BIOCHEM, France. Copper (II) nitrate trihydrate ($Cu(NO_3)_2.3H_2O$). Rhodamine B. All chemicals were utilized as obtained without additional purification. Distilled water was produced in the biology lab.

### Tools and Characterization:

Transmission electron microscopy was performed using a TEM JEOL JEM-1010, Japan. SEM/EDAX was performed using an SEM FEI Quanta 250 FEG, USA. X-ray diffraction (XRD) was performed utilizing a Bruker D8 Discover XRD (Germany) with Cu Kα radiation (λ = 0.154060 nm) over a 5° to 80° range, operating at 40 kV and 30 mA. Fourier Transform Infrared Spectroscopy (FTIR) was conducted using Japan's JASCO FT/IR-4000 spectrometer. Photoluminescence spectroscopy was performed using a custom-built fluorescence spectrophotometer with an adjustable light source and a spectrometer from SCEINCETECH9702 (Canada). UV-Vis absorption spectra were recorded with a CECIL CE 7200 spectrometer. A high-speed centrifuge model KT7-900 434 is provided by Heller International Trading Co., Ltd., located in Kenda, Germany. A magnetic stirrer, hot plate (HS-12, China), and pH meter (model PH3-3DW, China) were used. Teflon-lined Stainless steel (100 mL) autoclave. Finally, a Desktop Constant-temperature Drying Oven of the model (WHL/50HZ) (FAITHFUL, China) was used.

### Graphene oxide (GO) Preparation:

Graphene oxide (GO) was prepared using the Hummers' method (Chen *et al.*, 2013), as shown in Figure 1. The procedure covers multiple stages. Mix 0.5 g of Graphite powder, 0.25 g of $NaSO_3$, and 23 mL of $H_2SO_4$, and stir in an ice bath at 4 °C or below for 30 minutes. Then, 1.5 g of $KMnO_4$ was gradually incorporated into the solution while stirring in an ice bath for 1 hour. After that, the ice bath was eliminated, and the temperature was raised to 35 °C. After 30 minutes, the temperature was raised to 90 °C, and 25 mL of distilled water was gradually added to the solution dropwise. The solution changed from a greenish-black to a yellowish-brown color. Stirred continuously for 24 hr. at ambient temperature. Finally, 2 mL of 30% $H_2O_2$ was added to the solution to stop the reaction. The resultant mixture was diluted with a 37% HCl solution, then centrifuged at 10,000 rpm for 5 minutes and filtered using filtration papers. After removing the supernatant, the remainder was repeatedly cleaned with distilled water until the pH reached neutrality. The obtained graphene oxide was dried in an oven at 60 °C for 24 hours.

### Graphene Quantum Dots Preparation:

Strongly fluorescent GQDs were produced through a solvothermal approach from GO(Tian *et al.*, 2016). First, 0.5 grams of the produced GO powder was added to 30 mL of dimethylformamide (DMF) and mixed for 1 hour until the powder was entirely dispersed. The mixture was contained in a Teflon-lined autoclave with a 100 mL capacity and heated to 200 °C for 20 hours in an electronic oven. Upon reaching ambient temperature, the resulting yellowish-green solution underwent centrifugation at 10,000 rpm for 10 minutes to eliminate larger fragments. The residue was filtered using a 0.22 µm membrane filter to eliminate any residual larger fragments and improve the purity of the GQDs.

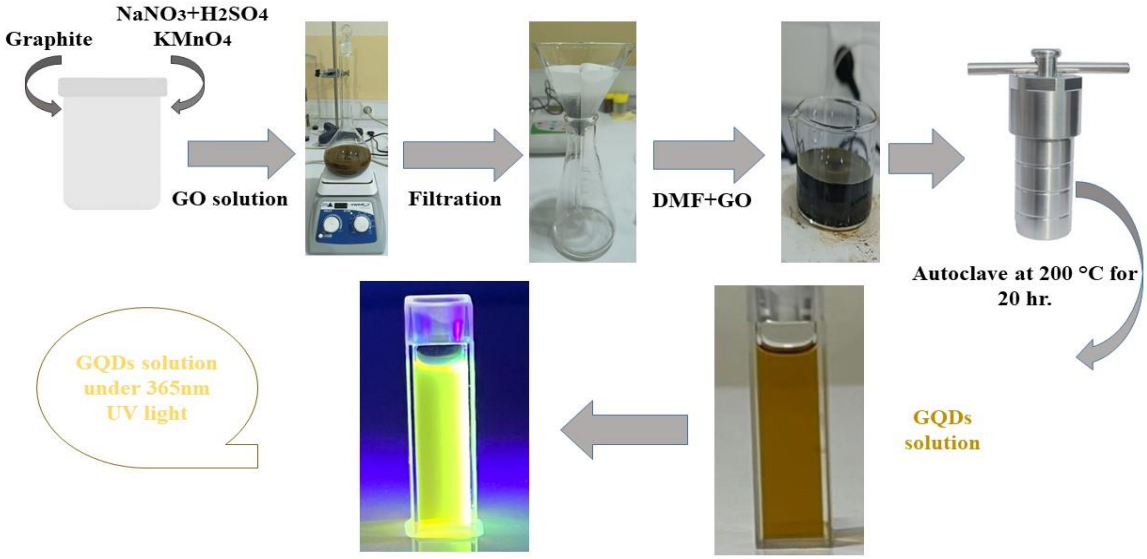


**Figure 1:** An illustration of the Hummers' technique used to synthesize GO and the solvothermal method for synthesizing GQDs.

### Fluorescence Measurements of Copper Ions:

The quantification of $Cu^{2+}$ ions was performed in aqueous solution under normal conditions. In the typical procedure, stock solutions of $Cu^{2+}$ ions were created by dispersing and diluting ($Cu(NO_3)_2.3H_2O$) in distilled water(Salih Ajaj *et al.*, 2023). A solution of GQDs was used as the sensing medium to detect $Cu^{2+}$ ions. A 3 mL sample of the GQD solution was placed in a quartz cuvette, after which solutions with various metal ions were added. The fluorescence intensity was then determined at a consistent excitation wavelength (500 nm). The PL properties of the GQDs were used to investigate their selectivity as sensors for various types of metal ions. The fluorescence intensity of the GQDs was examined at ambient temperature, and the GQDs' responsiveness to different metal ions was studied. Of all the tested ions, the $Cu^{2+}$ ion strongly reduced the GQDs` fluorescence; the PL intensities diminished progressively as the concentration of $Cu^{2+}$ ions increased, indicating that the GQDs could be applied as a sensitive luminescent probe for the selective identification of $Cu^{2+}$ ions.

### Optical Nanothermometry:

We investigated their temperature sensitivity to assess the potential use of GQD solutions in nano-thermometry. A quartz cuvette containing 3.5 mL GQD solution was set on a hot plate. The temperature was raised from 20 to 70 °C in 10 °C increments to take measurements. To guarantee accurate measurement, a thermometer was placed in the solution at each temperature. Photoluminescence spectra were taken using an excitation wavelength of 500 nm while maintaining thermal equilibrium.

### Quantum Yield Measurement for GQDs:

The quantum yield (QY) of the graphene quantum dots (GQDs) was measured using a single-point comparative method according to the equation below:

$$QY_{GQD} = QY_{ST} \times (F_{GQD}/F_{ST}) \times (A_{ST}/A_{GQD}) \times (\eta_{GQD}/\eta_{ST})^2$$

F refers to the total intensity of fluorescence, A denotes the absorbance, and η signifies the solvent's refractive index(Saber et al., 2024). Rhodamine B, with a reported quantum yield value (QY = 0.31 in water), was selected as the reference standard to evaluate the quantum yield of the GQD solution. The standard and sample should absorb and emit light in similar spectral regions, which is why we chose Rhodamine B and GQDs, as their absorption spectra overlap(Zheng et al., 2020). To prepare a 0.1 M Rhodamine B stock solution, accurately weigh 0.332 g of Rhodamine B powder and disperse it in 10 mL of distilled water. After that, 200 µL of GQDs solution was diluted by adding it to 3 mL of distilled water in a quartz cuvette. To minimize their absorption effects, the concentration was chosen to ensure that the absorbance in the 10 mm fluorescence cuvette remained under 0.1 at a 500 nm excitation wavelength for both the standard and sample. The fluorescence spectra for both were then acquired at this optimal wavelength, and the integrated fluorescence intensity was determined under the emission curve that extended from 490 to 620 nm.

## 3. RESULTS

### TEM and SEM Analysis of GQDs:

The structural properties of the produced GQDs were studied using SEM and TEM scanning approaches. The SEM image in Figure 2a, taken at a scale of 2 µm with a magnification of 20000, operated at a voltage of 30 kV, reveals an agglomerated structure, indicating the presence of densely packed quantum dots. This agglomeration is typical for nanomaterials due to van der Waals interactions. However, TEM analysis offered more accurate insights into the individual particle sizes and shapes of the GQDs. As shown in Figures 2b and 2c, a predominantly spherical shape with evenly distributed nanoparticles was observed. The GQDs display a consistent size distribution, with a typical particle diameter of 4.12 nm. According to the histogram in Figure 2(d), the most common particle diameter is

approximately 3.982 nm, with a size distribution ranging from 2.351 nm to 6.756 nm. The SEM and TEM analyses confirm that GQDs are nanometric, which is essential for their potential applications in sensors and optoelectronic devices.

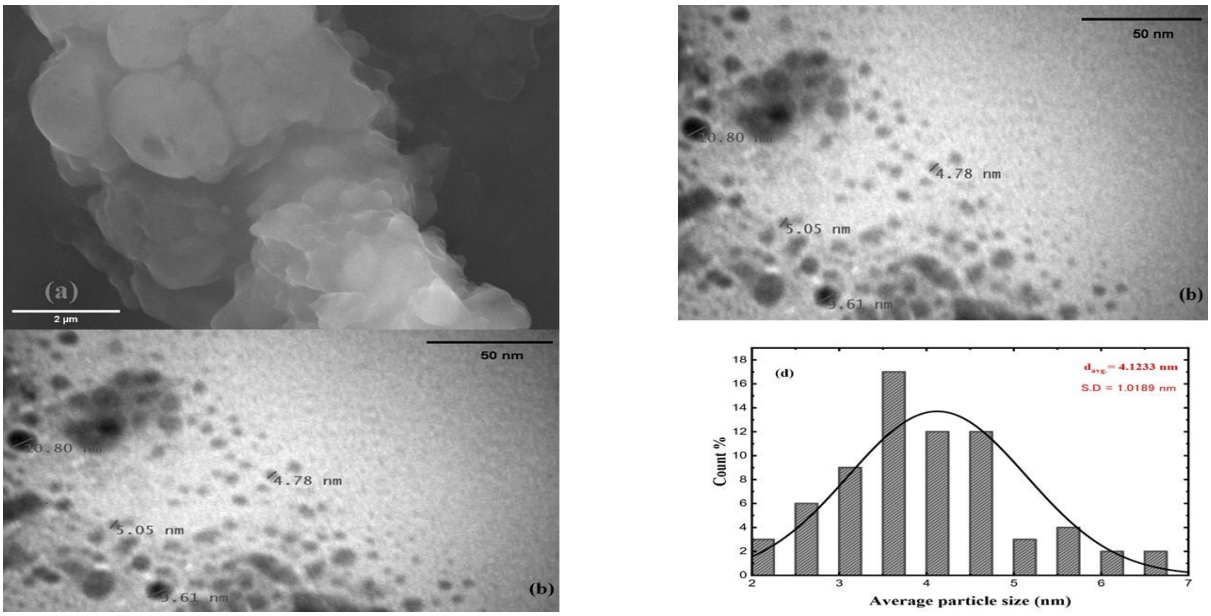


**Figure 2:** (a) shows an SEM image, (b) and (c) are TEM images captured at different magnifications of the synthesized GQDs, and (d) presents the corresponding particle size distribution histogram.

## Structural Characterization by XRD:

The synthesized GQDs were analyzed for their structural features utilizing X-ray diffraction (XRD). The XRD pattern of the sample, shown in Figure 3, exhibits a broad diffraction peak centered at 24.9° (2θ). This peak relates to the (002) plane of graphitic carbon with d-spacing (0.362 nm) calculated from Bragg`s equation (n λ=2dsin(θ)), indicating the presence of highly disordered and nanosized graphene domains, which is a characteristic feature of GQDs(Ahirwar *et al.*, 2017; Truong *et al.*, 2023). The observed shift from the typical graphite peak at approximately 26.5° suggests the existence of oxygen functional groups and highlights the effects of quantum confinement. The absence of distinct peaks indicates the amorphous characteristics of the synthesized GQDs, confirming their minimal dimensions and the disordered $sp^2$ carbon domains (Mahato *et al.*, 2023).

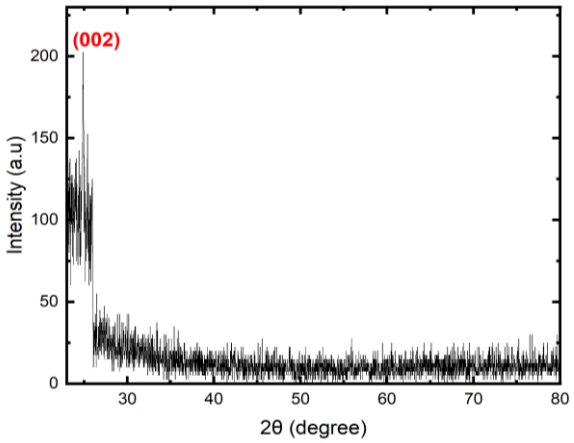


**Figure 3:** XRD patterns recorded for GQDs.

## Surface Chemistry and Chemical Composition Analysis:

FTIR spectroscopy, ranging from (4000-400) $cm^{-1}$, was used to evaluate the chemistry of GQDs. The FTIR spectrum in Figure 4a clearly shows O-H and N-H stretching vibrations at approximately 3495 $cm^{-1}$, likely derived from amine groups added by DMF or remaining hydroxyl (-OH) groups (Zhu *et al.*, 2011). A noticeable peak at approximately 3138 $cm^{-1}$ was observed, which is related to C–H stretching vibrations of $sp^2$ hybridized carbon atoms, typically present at the edges of aromatic domains(Truong *et al.*, 2023). The characteristic peak at approximately (1650–1750 $cm^{-1}$) proves the existence of carbonyl (C=O) or amide functionalities, implying partial oxidation or contributions from DMF decomposition(Chua *et al.*, 2015). The vibration of C=C bonds in $sp^2$-hybridized carbon atoms was observed at 1656 $cm^{-1}$, which is a signature feature of the graphene framework. A peak at 1496 $cm^{-1}$ appears, equivalent to the stretching of C=N and C–N bonds, confirming the incorporation of nitrogen into the GQD framework. Also, bands between (1093-1387 $cm^{-1}$) are defined as C–O–C and C–N stretching, further ensuring the existence of oxygen and nitrogen functional groups(Hasan *et al.*, 2019). Weak absorption below 900 $cm^{-1}$ implies aromatic C–H bending, indicating the graphene-like structure of the GQDs. The findings indicate that the produced GQDs exhibit nitrogen doping, with DMF serving as a nitrogen source while retaining oxygen functional groups, which enhances their dissolution in polar solvents (Pan et al., 2010a). The composition of the synthesized GQDs was examined using energy-dispersive X-ray spectroscopy (EDX). The spectrum displayed in Figure 4b verifies the presence of carbon (C), oxygen (O), and nitrogen (N), confirming the successful creation of nitrogen-doped GQDs (N-GQDs). The quantitative analysis indicates that carbon is the most abundant element, comprising 82.48% by weight, followed by oxygen at 10.53% and nitrogen at 6.99%. The significant carbon content suggests a graphitized structure, which is validated in the case of GQDs. Additionally, oxygen suggests that oxygen-containing functional groups are retained, which can optimize the material's hydrophilicity and surface reactivity. The detection of nitrogen in the sample, likely introduced during the solvothermal synthesis using N, N-dimethylformamide (DMF), confirms successful nitrogen doping.

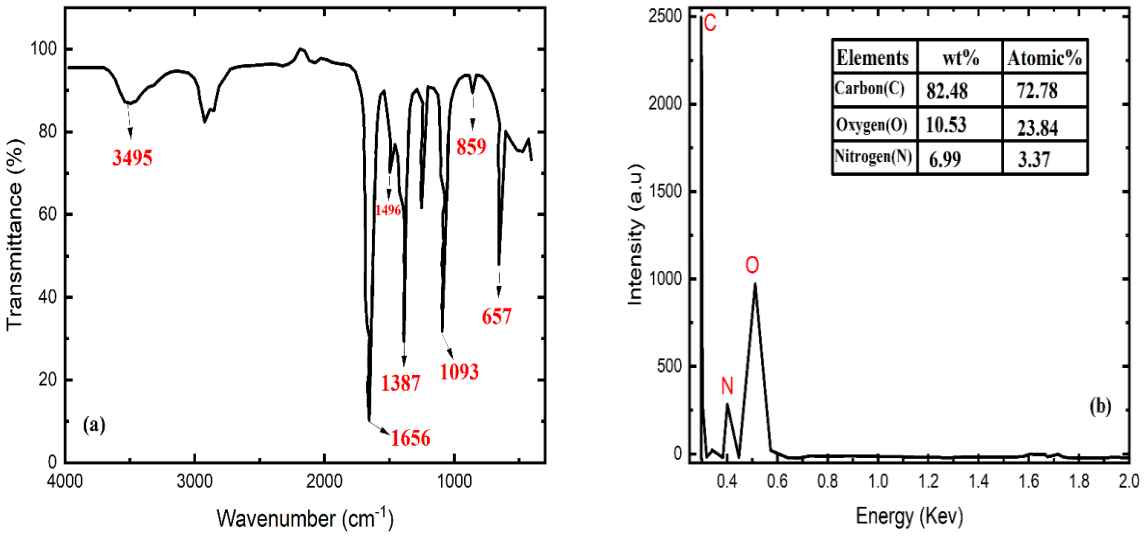


**Figure 4:** (a) FTIR and (b) EDX spectra for the prepared GQDs.

## OPTICAL PROPERTIES OF GQDs

### Photoluminescence (PL) Analysis of GQDs:

The PL spectrum of the produced GQDs was taken over excitation wavelengths from 400 nm to 530 nm, as illustrated in Figure 5. The emission profile exhibits a pronounced dependence on the excitation wavelength, a typical characteristic of GQDs(Truong *et al.*, 2023). At lower excitation wavelengths (400–420 nm), emission peaks are seen at shorter wavelengths (~480–500 nm). Conversely, raising the excitation wavelength causes the emission maxima to shift to longer wavelengths around (550–580 nm), which is a redshift. This behavior is attributed to excitation resulting from various emissive states in the GQDs, induced by quantum confinement effects and surface defects (Shen *et al.*, 2011). The peak photoluminescence intensity was taken at an excitation wavelength of 500 nm, yielding a maximum emission at 551 nm (strong green emission). The broad emission profile indicates a distribution of $sp^2$ domains of varying sizes and oxygen functional groups on the GQD surface (Sun *et al.*, 2013).

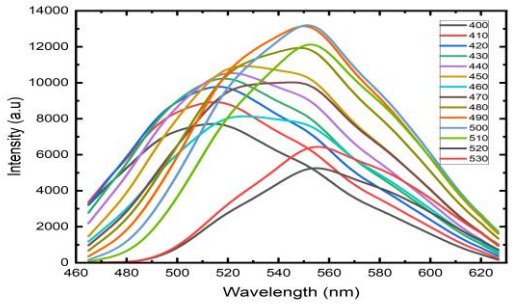


**Figure 5:** Photoluminescence emission spectra of GQDs at various excitation wavelengths.

### UV-Visible Spectroscopy:

UV-Vis spectroscopy was used to examine the optical properties of the produced GQDs, as shown in Figure 6. The absorption spectrum presents a noticeable peak at 273 nm, consistent with the π–π* transition of the C=C bonds within the $sp^2$-hybridized carbon framework(Dong *et al.*, 2012). The absorption intensity slowly decreases with increasing wavelength, extending into the visible region. This behavior is typical for GQDs, caused by their quantum confinement and edge effects(Qu *et al.*, 2013). The weak absorbance at long wavelengths implies that there are oxygen species or low-coordinated carbon atoms, which can lead to additional n–π* transitions on the surfaces(Wang *et al.*, 2014).

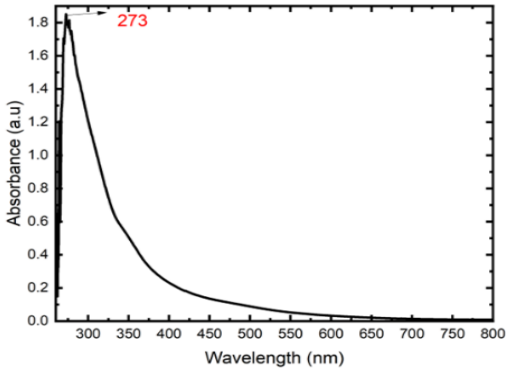


**Figure 6:** UV-visible absorption spectra of GQDs.

## APPLICATIONS OF GQDs

### Detection of Cu2+ ions:

The selective response of graphene quantum dot (GQD) fluorescence for different metal ions was studied. In this test, GQDs were exposed to a range of cations and anions, including $Ti^{4+}$, $Ag^{+}$, $Zn^{2+}$, $Cd^{2+}$, $Na^{+}$, $K^{+}$, $Cu^{2+}$, $Cl^{-}$, $SO4^{2-}$, and $NO3^{-}$. The concentration of each ion solution was 190.2 mM, and the measurements were performed under 500 nm excitation Figure 7a. It was clear that, except for $Cu^{2+}$, the other ions investigated had no apparent quenching abilities towards the PL of GQD. The results indicate that the nanomaterial exhibits a highly selective adsorption towards copper ions. We quantified $Cu^{2+}$ ions based on the fluorescence intensity changes of the obtained GQDs in response to varying concentrations of $Cu^{2+}$ ions added to the GQD solution. The fluorescence intensity of the GQDs decreased upon the addition of $Cu^{2+}$ to the solution(Zu *et al.*, 2017a). To measure this sensing behavior, gradual additions of $Cu^{2+}$ (0.09–0.19 μM) were introduced into the GQD suspension, and the resulting decrease in emission intensity was recorded (Figure 7b).

A significant, concentration-dependent quenching was noted. The linear decrease in fluorescence intensity with $Cu^{2+}$ concentration (Figure 7c) further supports this observation. The Stern-Volmer plot (Figure 7d) shows a strong linear relationship ($R^2$ = 0.9305), confirming that the quenching behavior follows Stern-Volmer kinetics. This behavior is characteristic of a dynamic quenching mechanism, where $Cu^{2+}$ ions collide with excited GQDs, facilitating non-radiative relaxation. However, the significant decrease in PL with concentration, along with the Stern-Volmer behavior, indicates that dynamic (collisional) quenching is the dominant mechanism(Iqbal *et al.*, 2016; Zu *et al.*, 2017b). The limits of detection (LoD) and quantification (LoQ) were calculated as **0.55 µM** and 1.6 µM, respectively(Fu *et al.*, 2017). The observed visual change under UV light (Figure 7e) from bright emission to quenched fluorescence further supports its sensing capability.

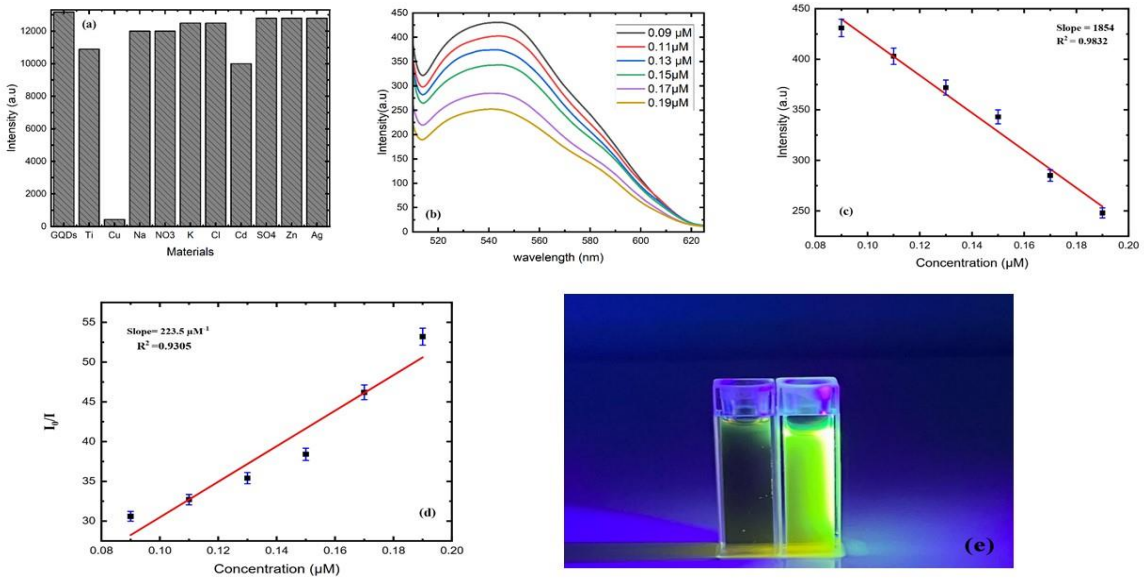


**Figure 7:** (a) A bar chart illustrating the PL strength of GQDs after the inclusion of various materials, highlighting their selectivity for $Cu^{2+}$ ions, (b) Variation in photoluminescence intensity of graphene quantum dots based on different $Cu^{2+}$ ion concentrations, demonstrating the quenching behavior, (c) The relation between the PL intensity of GQDs and varying concentrations of $Cu^{2+}$ ions, (d) A Stern-Volmer plot illustrating the quenching process and the sensor's response, (e) Images of GQD solutions taken under 365 nm UV light before (right) and after (left) the addition of $Cu^{2+}$ ions.

## GQD-Based Optical Nanothermometer:

We further investigated the temperature-dependent fluorescence characteristics of the graphitic carbon dots (GDs) to assess their potential as temperature sensors. Figure 8a presents the temperature-dependent PL spectra of the GQDs, measured at an excitation wavelength of 500 nm. As the temperature rose from 20 °C to 70 °C, we observed a gradual decrease in fluorescence intensity at the emission peak of 551 nm with no significant shift in the emission wavelength. A linear fit of the PL intensity versus temperature yielded a slope of -69.5 a.u./°C and a determination coefficient ($R^2$) of 0.94936, indicating a strong linear relationship, as shown in Figure 8b. The relative temperature sensitivity was calculated at 70 °C ($S_R$) of **1.81 % °C$^{-1}$.**

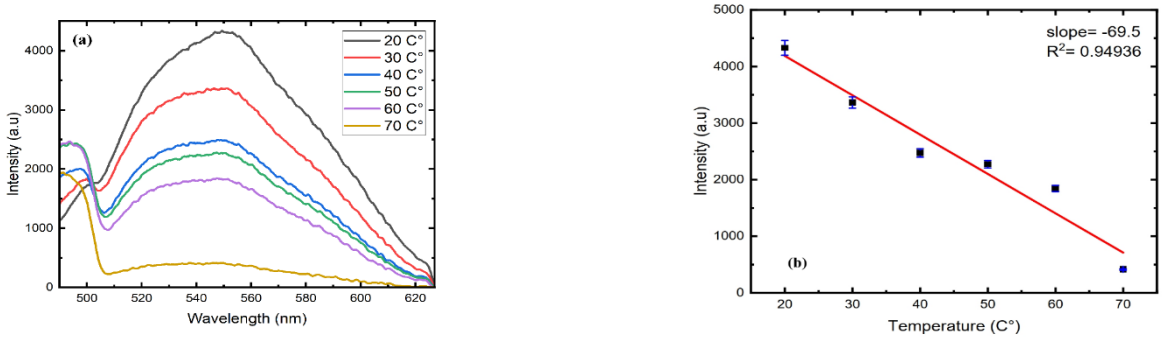


**Figure 8:** (a) The emission spectrum of GQD dispersion through a temperature range of 20 to 70 °C; (b) The correlation between PL intensity and temperature.

## 3. DISCUSSION

This research used a solvothermal process to synthesize graphene quantum dots from graphene oxide as the starting material, utilizing DMF as both the solvent and a source of nitrogen. The extended solvothermal treatment at 200 °C for 20 hours appears to have significantly impacted the optical and structural properties of the produced GQDs. In comparison to related studies, where reaction durations usually span from 4 to 12 hours, the longer time in this research probably facilitated more thorough carbonization and the passivation of oxygen-containing functional groups. TEM analysis revealed that the produced GQDs had a predominantly spherical form with an average diameter of 4.12 nm, and the majority of the particles had a size of approximately 3.982 nm. The size distribution ranges from 2.351 nm to 6.756 nm, indicating the high-efficiency fragmentation of the GO into nanometer-sized domains. The uniform size distribution implies that the nucleation and growth process is well-controlled, which is probably contributed to by the long solvothermal treatment at 200 °C for 20 hours and the use of DMF as the solvent. The XRD pattern of the starting material, graphene oxide (GO), from previous reports shows a diffraction peak at (~10.65º) with indices (001) and an interlayer spacing (d) of 0.817 nm due to the increased interlayer spacing from oxygen-containing groups(Surekha *et al.*, 2020; Truong *et al.*, 2023). In contrast, the XRD pattern of GQDs shows a notable peak at approximately 24.9° (2θ), which corresponds to the (002) plane of graphitic carbon. This indicates both reduced crystallinity and a small particle size. The absence of the GO peak in the GQDs suggests that successful exfoliation and reduction occurred during the synthesis process. These findings are consistent with earlier studies on solvothermally synthesized GQDs (Yu *et al.*, 2017). The FTIR spectrum confirmed the presence of functional groups on the surface, such as carbonyl and hydroxyl, which enhance the water dispersibility and metal ion interaction of the GQD, a property necessary for $Cu^{2+}$ ion sensing. These results were consistent with EDX analysis, which revealed a large amount of carbon, along with the remaining oxygen and nitrogen, suggesting a partial reduction of GO. The lack of metallic impurities further suggests the high purity of the GQDs (Qi *et al.*, 2018). In this work, GQDs exhibited vigorous PL intensity, with a maximum emission peak located at 551 nm upon excitation at 500 nm, indicating green fluorescence emission. The emission is attributed to a quantum confinement effect, along with surface states influenced by oxygen-containing functional groups(Carrera *et al.*, 2025). The relatively high quantum yield of 51.56% indicates efficient radiative recombination and fewer nonradiative recombination pathways, which is attributed to the optimized surface passivation achieved through the extended solvothermal process. This value is significantly higher than most previously reported values for GQDs prepared using hydrothermal or solvothermal methods. (Table 1) shows that numerous previous studies have reported quantum yields (QYs) ranging from 10.3% to 49.1%, with only a few exceeding 30%. In this study, the achieved QY of **51.56%** indicates a significant improvement, showcasing the effectiveness of the DMF-assisted solvothermal method in producing high-quality, highly emissive GQDs.

**Table 1:** Comparison of the quantum yield values of GQDs synthesized using various precursors, solvents, and methods reported in prior studies.

| Precursor | Synthesis- method | Quantum-Yield (%) | Ref. |
|---|---|---|---|
| Cynodon Dactylon | Solvothermal | 49.1 | (Pai *et al.*, 2022) |
| Leaves of the curry tree | Hydrothermal | 14.4 | (Singh *et al.*, 2022) |
| Watermelon rind waste | Hydrothermal | 37 | (Rodwihok *et al.*, 2022) |
| Mangifera Indica leaf extract | Microwave-assisted | 10.3 | (Singh *et al.*, 2025) |
| 2,7-DHN & PA | Solvothermal | 24.9 | (Jin *et al.*, 2023) |
| Star anise fruit | Microwave-assisted | 16.52 | (Harde *et al.*, 2025) |
| Graphene oxide | Hydrothermal | 46 | (Su *et al.*, 2020) |
| GO | Solvothermal | 51.56 | This study |

The characteristic absorbance shoulder appears at approximately 270-280 nm of UV–Vis evident π–π* transition band of carbonyl or hydroxyl groups, confirming the existence of both aromatic domains and functional surface groups(Wang *et al.*, 2014; Zhu *et al.*, 2015). The excitation-dependent emission property of these GQDs also lends strength to the fact that there is more than one emissive trap present on the surface, as expected for GQDs prepared from graphene oxide. The high quantum yield, stable green emission, and excitation-dependent properties of the GQDs qualify these GQDs as highly sensitive copper ion sensors and nanothermometers. The obtained GQD was used to fabricate an ultrasensitive copper ion sensor. A notable reduction in fluorescence intensity was detected following the addition of $Cu^{2+}$, because of the electrons or energy transfer from GQDs to $Cu^{2+}$. The closer proximity of surface functional groups of the GQDs to $Cu^{2+}$ is efficacious in improving the quenching effect for selective and efficient sensing. (Table 2) compares the limit of detection (LoD) values for ion sensing applications of the synthesized GQDs with those reported in previous studies. These studies involved GQDs modified with various precious materials, demonstrating that our GQDs exhibit competitive or superior sensitivity.

**Table 2:** Summary of selected GQD-based ion sensors reported in the previous studies, including Precursor, target ions, and limits of detection (LOD).

| Precursor | Target ion | LoD | Ref. |
|---|---|---|---|
| Watermelon rind waste | $Fe^{3+}$ | 0.28 µM | (Rodwihok *et al.*, 2022) |
| P-coumaric acid | $Cu^{2+}$ | 57 $nML^{-1}$ | (Gao *et al.*, 2020) |
| Citric acid | $Cl^{-}$ | 10 mM | (Ifrah *et al.*, 2022) |
| Citric acid | $As^{3+}$ | 13 nM | (Mohagheghpour *et al.*, 2024) |
| Citric acid & L-cysteine | $Hg^{2+}$ | 0.239 nM | (Naksen *et al.*, 2025) |
| GO | $Cu^{2+}$ | 0.55 µM | This study. |

Moreover, the temperature sensitivity of the PL emission of the GQDs rendered them highly efficient nanothermometers. The decrease in PL intensity of GQDs with increasing temperature suggests a thermally activated non-radiative

relaxation mechanism. This behavior may be due to phonon-assisted relaxation, thermal expansion of trap states, and surface state dynamics. The linear PL quenching trend and solution-phase synthesis, which create surface defects and oxygen-containing groups, indicate that phonon-assisted recombination and temperature-induced surface changes mainly drive the nanothermometric response. Similar findings have been noted in studies on carbon-based nanomaterials(Li *et al.,* 2015; Ye *et al.*, 2021). This high sensitivity and good linearity confirm the potential of GQDs to serve as efficient and reliable nano-thermometers for optical temperature sensing applications. Table 3 compares the temperature sensitivity values of our synthesized GQDs with those reported in previous studies, indicating their promising performance for nanothermometer applications.

**Table 3:** Fluorescent graphene dots are affected by temperature.

| Precursor | Linear range | Temperature sensitivity | References |
|---|---|---|---|
| rGO | (296–373) K | 0.98% $K^{-1}$ | (Sehrawat & Islam, 2019) |
| rGO | (300-77) K | 1999.8% $K^{-1}$ | (Sehrawat & Islam, 2019) |
| Glucosamine | (25–45) °C | - | (Lee *et al.*, 2021) |
| Citric acid | (5-75) °C | 0.41% $°C^{-1}$ | (Zhang *et al.*, 2019) |
| GO | (20-70) °C | 1.81 % $°C^{-1}$ | This study. |

## CONCLUSION

This research focused on producing graphene quantum dots (GQDs) via a one-step solvothermal method using graphene oxide in dimethylformamide (DMF). The resulting particles had an average diameter of 4.1 nm and exhibited a high quantum yield of 51.6% when excited at 500 nm. Comprehensive characterization methods, including TEM, SEM, EDX, XRD, FTIR, UV-Vis spectroscopy, and photoluminescence spectroscopy, confirmed the preservation of the graphene framework, the integration of oxygen functional groups on the surface, and the strong, tunable emission behavior of the GQDs. With a sub-micromolar LoD and a linear Stern-Volmer quenching range of 0.09–0.19 µM, these DMF-derived GQDs demonstrate exceptional selectivity and sensitivity for $Cu^{2+}$ ions. Additionally, temperature-dependent photoluminescence (PL) measurements reveal a relative sensitivity of 1.81% $°C^{-1}$ over a temperature range of 20–70 °C, highlighting their potential as effective nanothermometers suitable for small-scale thermal sensing applications. The photoluminescent response of the synthesized GQDs for copper ion detection and temperature variation demonstrates their potential as dual-mode sensors. Although the sensing modes were studied separately, their optical stability suggests applicability in real-time multifunctional sensing platforms. The integration of ion detection and thermal sensing in a single nanostructure could reduce sample requirements, enhance analytical throughput, and improve spatial resolution for real-time applications. This dual functionality could enable the simultaneous monitoring of metal ion concentrations and temperature fluctuations in biological or environmental contexts, which is essential for applications such as intracellular diagnostics, water quality monitoring, or wearable sensing systems. Future work may focus on integrating and optimizing both sensing modes within a single system to improve real-time performance and reduce cross-sensitivity.

## Acknowledgement

The authors would like to express their sincere gratitude to the Physics Research Center at the University of Zakho for providing the necessary laboratory facilities and support to conduct this research.

## Contribution of Authors

Sitya Hishyar Ali conducted the experimental work, performed the data analysis, and prepared the manuscript.
Diyar Sadiq contributed to supervision, interpretation of results, and critical revision of the manuscript.
All authors reviewed and approved the final version of the manuscript.

## Ethical Statement

The authors confirm that this research did not involve any human or animal subjects.

## Funding

The authors declare that no funding was received for this study.

## REFERENCES

Ahirwar, S., Mallick, S., & Bahadur, D. J. A. o. (2017). Electrochemical method to prepare graphene quantum dots and graphene oxide quantum dots. *ACS Omega*, *2*(11), 8343-8353. https://doi.org/http://dx.doi.org/10.1021/acsomega.7b01539

Allahbakhsh, A., & Bahramian, A. R. J. J. o. M. L. (2018). Self-assembly of graphene quantum dots into hydrogels and cryogels: Dynamic light scattering, UV–Vis spectroscopy and structural investigations. *Journal of Molecular Liquids*, *265*, 172-180. https://doi.org/https://doi.org/10.1016/j.molliq.2018.05.123

Bayat, A., & Saievar-Iranizad, E. J. J. o. L. (2017). Synthesis of green-photoluminescent single layer graphene quantum dots: Determination of HOMO and LUMO energy states. *Journal of Luminescence*, *192*, 180-183. https://doi.org/https://doi.org/10.1016/j.jlumin.2017.06.055

Carrera, C., Galán-González, A., Maser, W. K., & Benito, A. M. J. C. S. (2025). Multifaceted role of H 2 O 2 in the solvothermal synthesis of green-emitting nitrogen-doped graphene quantum dots. *ChemicalScience*. https://doi.org/https://doi.org/10.1039/D4SC07896A

Chen, J., Yao, B., Li, C., & Shi, G. J. C. (2013). An improved Hummers method for eco-friendly synthesis of graphene oxide. *Carbon*, *64*, 225-229. https://doi.org/https://doi.org/10.1016/j.carbon.2013.07.055

Chua, C. K., Sofer, Z., Simek, P., Jankovsky, O., Klimova, K., Bakardjieva, S.,…Pumera, M. J. A. N. (2015). Synthesis of strongly fluorescent graphene quantum dots by cage-opening buckminsterfullerene. *ACS Nano*, *9*(3), 2548-2555. https://doi.org/https://pubs.acs.org/doi/10.1021/nn505639q

Dong, Y., Chen, C., Zheng, X., Gao, L., Cui, Z., Yang, H.,…Li, C. M. J. J. o. M. C. (2012). One-step and high yield simultaneous preparation of single-and multi-layer graphene quantum dots from CX-72 carbon black. *Journal of Materials Chemistry*, *22*(18), 8764-8766. https://doi.org/https://doi.org/10.1039/C2JM30658A

Fan, C., Yang, R., Huang, Y., Mao, L., Yang, Y., Gong, L.,…Zhong, L. J. J. o. E. C. (2023). Graphene quantum dots as sulfiphilic and lithiophilic mediator toward high stability and durable life lithium-sulfur batteries. *Journal of Energy Chemistry*, *85*, 254-266.

https://doi.org/https://doi.org/10.1016/j.jechem.2023.06.030

Fan, Z., Li, S., Yuan, F., & Fan, L. J. R. A. (2015). Fluorescent graphene quantum dots for biosensing and bioimaging. *RSC Advances*, *5*(25), 19773-19789. https://doi.org/https://doi.org/10.1039/C4RA17131D

Fu, H., Ji, Z., Chen, X., Cheng, A., Liu, S., Gong, P.,…chemistry, b. (2017). A versatile ratiometric nanosensing approach for sensitive and accurate detection of Hg 2+ and biological thiols based on new fluorescent carbon quantum dots. *Analytical and Bioanalytical Chemistry*, *409*, 2373-2382. https://doi.org/https://doi.org/10.1007/s00216-017-0183-3

Gao, B., Chen, D., Gu, B., Wang, T., Wang, Z., Yang, Y.,…Wang, G. J. C. A. P. (2020). Facile and highly effective synthesis of nitrogen-doped graphene quantum dots as a fluorescent sensing probe for Cu2+ detection. *20*(4), 538-544. https://doi.org/https://doi.org/10.1016/j.cap.2020.01.018

Harde, M. T., Lakade, S., Patokar, S., More, M. P., Joshi, S., Lodha, S.,…Nangare, S. J. J. o. F. (2025). Green-Synthesized Hyaluronic Acid-Conjugated Fluorescent Graphene Quantum Dots for Bioimaging and Cancer Theranostics: Synthesis, Characterization, and Cytotoxicity Assessment. *Journal of Fluorescence*, 1-14. https://doi.org/https://doi.org/10.1007/s10895-025-04388-7

Hasan, M. T., Gonzalez-Rodriguez, R., Ryan, C., Pota, K., Green, K., Coffer, J. L., & Naumov, A. V. J. N. R. (2019). Nitrogen-doped graphene quantum dots: Optical properties modification and photovoltaic applications. *Nano Research*, *12*, 1041-1047. https://doi.org/https://doi.org/https://doi.org/10.1007/s12274-019-2337-4.

Hsieh, C.-T., Sung, P.-Y., Gandomi, Y. A., Khoo, K. S., & Chang, J.-K. J. C. (2023). Microwave synthesis of boron- and nitrogen-codoped graphene quantum dots and their detection to pesticides and metal ions. *Chemosphere*, *318*, 137926. https://doi.org/https://doi.org/10.1016/j.chemosphere.2023.137926

Ifrah, Z., Shah Rukh, A., Muhammad Nauman, S., Maryam, S., & Rahat, U. J. F. i. M. (2022). Fluorescence quenching of graphene quantum dots by chloride ions: A potential optical biosensor for cystic fibrosis. *Frontiers in Materials*, *9*, 857432. https://doi.org/https://doi.org/10.3389/fmats.2022.857432

Iqbal, A., Tian, Y., Wang, X., Gong, D., Guo, Y., Iqbal, K.,…Chemical, A. B. (2016). Carbon dots prepared by solid state method via citric acid and 1, 10-phenanthroline for selective and sensing detection of Fe2+ and Fe3+. *Sensors and Actuators B: Chemical*, *237*, 408-415. https://doi.org/http://dx.doi.org/doi:10.1016/j.snb.2016.06.126

Jiang, D., Chen, Y., Li, N., Li, W., Wang, Z., Zhu, J.,…Xu, S. J. P. O. (2015). Synthesis of luminescent graphene quantum dots with high quantum yield and their toxicity study. *PLOS one*, *10*(12), e0144906. https://doi.org/https://doi.org/10.1371/journal.pone.0144906

Jin, X.-J., Tan, L., Zhao, Z.-Q., Li, M.-C., Zhou, Q.-Y., Zhang, J.-J., Zeng, Z. J. N. J. o. C. (2023). Facile synthesis of graphene quantum dots with red emission and high quantum yield. *New Journal of Chemistry*, *47*(5), 2221-2229. https://doi.org/https://doi.org/10.1039/D2NJ04491A

Jin, Z., Owour, P., Lei, S., Ge, L. J. C. O. i. C., & Science, I. (2015). Graphene, graphene quantum dots and their applications in optoelectronics. *Current Opinion in Colloid & Interface Science*, *20*(5-6), 439-453. https://doi.org/https://doi.org/10.1016/j.cocis.2015.11.007

Kharangarh, P. R., Ravindra, N. M., Singh, G., & Umapathy, S. J. E. S. (2023). Synthesis of luminescent graphene quantum dots from biomass waste materials for energy-related applications—an Overview. *Energy Storage*, *5*(3), e390. https://doi.org/https://doi.org/10.1002/est2.390

Kharangarh, P. R., Singh, G. J. E. J. o. S. S. S., & Technology. (2023). Effect of Mo-doped strontium cobaltite on graphene nanosheets for creating a superior electrode in supercapacitor applications. *ECS Journal of Solid State Science and Technology*, *12*(3), 031006. https://doi.org/DOI 10.1149/2162-8777/acc095

Krishnan, S. K., Singh, E., Singh, P., Meyyappan, M., & Nalwa, H. S. J. R. a. (2019). A review on graphene-based nanocomposites for electrochemical and fluorescent biosensors. *RSC Advances*, *9*(16), 8778-8881. https://doi.org/https://doi.org/10.1039/C8RA09577A

Kurniawan, D., Anjali, B. A., Setiawan, O., Ostrikov, K. K., Chung, Y. G., Chiang, W.-H. J. A. A. M., & Interfaces. (2021). Microplasma band structure engineering in graphene quantum dots for sensitive and wide-range pH sensing. *ACS Applied Materials & Interfaces*, *14*(1), 1670-1683. https://doi.org/https://pubs.acs.org/doi/10.1021/acsami.1c18440

Lee, B. H., McKinney, R. L., Hasan, M. T., & Naumov, A. V. J. M. (2021). Graphene quantum dots as intracellular imaging-based temperature sensors. *Materials*, *14*(3), 616. https://doi.org/https://doi.org/10.3390/ma14030616

Li, X., Rui, M., Song, J., Shen, Z., & Zeng, H. J. A. F. M. (2015). Carbon and graphene quantum dots for optoelectronic and energy devices: a review. *Advanced Functional Materials*, *25*(31), 4929-4947. https://doi.org/https://doi.org/10.1002/adfm.201501250

Lin, L., & Zhang, S. J. C. c. (2012). Creating high yield water soluble luminescent graphene quantum dots via exfoliating and disintegrating carbon nanotubes and graphite flakes. *Chemical Communications*, *48*(82), 10177-10179. https://doi.org/https://doi.org/10.1039/C2CC35559K

Mahato, P. K., Choudhuri, S., Kumar, C., Roy, S., & Patra, P. J. M. T. P. (2023). Evaluation of crystal size present in graphene oxide quantum dots using optical and Raman spectroscopy. *materialstoday: PROCEEDINGS*, *80*, 668-673. https://doi.org/https://doi.org/10.1016/j.matpr.2022.11.066

Martins, G., Galvan, A. L. S., Valenga, M. G., Cardozo Martins, T. A., Bergamini, M. F., & Marcolino-Junior, L. H. J. A. A. N. M. (2025). Nitrogen-Doped Graphene Quantum Dots (N-GQDs): A Promising Material for the Development of Electrochemical Immunosensors. *ACS Applied Nano Materials*. https://doi.org/https://pubs.acs.org/doi/10.1021/acsanm.4c06568

Mohagheghpour, E., Farzin, L., & Sadjadi, S. J. B. T. E. R. (2024). Alendronate-functionalized graphene quantum dots as an effective fluorescent sensing platform for arsenic Ion detection. *Biological Trace Element Research*, *202*(5), 2391-2401. https://doi.org/https://doi.org/10.1007/s12011-023-03819-5

Naksen, P., Khamlam, P., Khemthong, P., Yodsin, N., Phanthasri, J., Youngjan, S.,…Samphao, A. J. M. J.

(2025). Nitrogen and sulfur doped graphene quantum dots as a fluorometric paper-based sensor for highly selective and sensitive detection of mercury ions in aqueous samples. *Microchemical Journal*, 114623. https://doi.org/https://doi.org/10.1016/j.microc.2025.114623

Novoselov, K. S., Geim, A. K., Morozov, S. V., Jiang, D.-e., Zhang, Y., Dubonos, S. V.,…Firsov, A. A. J. s. (2004). Electric field effect in atomically thin carbon films. *Sceince*, *306*(5696), 666-669. https://doi.org/https://doi.org/10.1126/science.1102896

Pai, A. R., Sasi, B. S., Arya, J., & Arjun, K. (2022). Synthesis of Graphene Quantum dots from the fresh leaves extract of Cynodon Dactylon and its Photoluminescence studies. IOP Conference Series: Materials Science and Engineering, doi:10.1088/1757-899X/1219/1/012005

Pan, D., Zhang, J., Li, Z., & Wu, M. J. A. m. (2010a). Hydrothermal route for cutting graphene sheets into blue-luminescent graphene quantum dots. *ADVANCED MATERIALS*, *22*(6), 734-738. https://doi.org/DOI: 10.1002/adma.200902825

Pan, D., Zhang, J., Li, Z., & Wu, M. J. A. m. (2010b). Hydrothermal route for cutting graphene sheets into blue-luminescent graphene quantum dots. *ADVANCED MATERIALS*, *22*(6), 734-738. https://doi.org/DOI: 10.1002/adma.200902825

Qi, B.-P., Zhang, X., Shang, B.-B., Xiang, D., & Zhang, S. J. J. o. N. R. (2018). Solvothermal tuning of photoluminescent graphene quantum dots: from preparation to photoluminescence mechanism. *Journal of Nanoparticle Research*, *20*, 1-9. https://doi.org/https://doi.org/10.1007/s11051-018-4123-8

Qu, D., Zheng, M., Du, P., Zhou, Y., Zhang, L., Li, D.,…Sun, Z. J. N. (2013). Highly luminescent S, N co-doped graphene quantum dots with broad visible absorption bands for visible light photocatalysts. *Nanoscale*, *5*(24), 12272-12277. https://doi.org/https://doi.org/10.1039/C3NR04402E

Rajender, G., Choudhury, B., & Giri, P. J. N. (2017). In situ decoration of plasmonic Au nanoparticles on graphene quantum dots-graphitic carbon nitride hybrid and evaluation of its visible light photocatalytic performance. *Nanotechnology*, *28*(39), 395703. https://doi.org/DOI 10.1088/1361-6528/aa810a

Reghunath, B. S., Rajasekaran, S., KR, S. D., Pinheiro, D., & UC, J. R. J. J. I. J. o. H. E. (2023). N-doped graphene quantum dots incorporated cobalt ferrite/graphitic carbon nitride ternary composite for electrochemical overall water splitting. *International Journal of Hydrogen Energy*, *48*(8), 2906-2919. https://doi.org/https://doi.org/10.1016/j.ijhydene.2022.10.169

Rodwihok, C., Tam, T. V., Choi, W. M., Suwannakaew, M., Woo, S. W., Wongratanaphisan, D., & Kim, H. S. J. N. (2022). Preparation and characterization of photoluminescent graphene quantum dots from watermelon rind waste for the detection of ferric ions and cellular bio-imaging applications. *Nanomaterials*, *12*(4), 702. https://doi.org/https://doi.org/10.3390/nano12040702

Saber, Y. A., Hamed, M., Emara, S., Mansour, F. R., Locatelli, M., & Ibrahim, N. J. H. (2024). Garlic peel-based carbon quantum dots as a sustainable alternative for the sensitive and green spectrofluorometric quantification of molnupiravir in pharmaceutical capsules. *Heliyon*, *10*(23). https://doi.org/https://doi.org/10.1016/j.heliyon.2024.e40661

Salih Ajaj, C., Sadiq, D. J. N., & Nanotechnology. (2023). Mulberry Juice-Derived Carbon Quantum Dots as a Cu2+ Ion Sensor: Investigating the Influence of Fruit Ripeness on the Optical Properties. *Nanomaterials and Nanotechnology*, *2023*(1), 9980479. https://doi.org/https://doi.org/10.1155/2023/9980479

Sehrawat, P., & Islam, S. J. N. A. (2019). An ultrafast quantum thermometer from graphene quantum dots. *Nanoscale Advances*, *1*(5), 1772-1783. https://doi.org/https://doi.org/10.1039/C8NA00361K

Shen, J., Zhu, Y., Chen, C., Yang, X., & Li, C. J. C. c. (2011). Facile preparation and upconversion luminescence of graphene quantum dots. *Chemical Communications*, *47*(9), 2580-2582. https://doi.org/https://doi.org/10.1039/C0CC04812G

Shen, J., Zhu, Y., Yang, X., & Li, C. J. C. c. (2012). Graphene quantum dots: emergent nanolights for bioimaging, sensors, catalysis and photovoltaic devices. *Chemical Communications*, *48*(31), 3686-3699. https://doi.org/https://doi.org/10.1039/C2CC00110A

Shi, M., Zhu, H., Chen, C., Jiang, J., Zhao, L., Yan, C. J. I. J. o. M., Metallurgy, & Materials. (2023). Synergistically coupling of graphene quantum dots with Zn-intercalated MnO2 cathode for high-performance aqueous Zn-ion batteries. *International Journal of Minerals, Metallurgy and Materials*, *30*(1), 25-32. https://doi.org/https://doi.org/10.1007/s12613-022-2441-4

Shin, Y., Lee, J., Yang, J., Park, J., Lee, K., Kim, S.,…Lee, H. J. S. (2014). Mass production of graphene quantum dots by one-pot synthesis directly from graphite in high yield. *communications*, *10*(5), 866-870. https://doi.org/DOI: 10.1002/smll.201302286

Shin, Y., Park, J., Hyun, D., Yang, J., Lee, J.-H., Kim, J.-H., & Lee, H. J. N. (2015). Acid-free and oxone oxidant-assisted solvothermal synthesis of graphene quantum dots using various natural carbon materials as resources. *Nanoscale*, *7*(13), 5633-5637. https://doi.org/https://doi.org/10.1039/C5NR00814J

Singh, A. K., Sri, S., Garimella, L. B., Dhiman, T. K., Sen, S., & Solanki, P. R. J. A. A. B. M. (2022). Graphene quantum dot-based optical sensing platform for aflatoxin B1 detection via the resonance energy transfer phenomenon. *ACS Applied Bio Materials*, *5*(3), 1179-1186. https://doi.org/https://pubs.acs.org/doi/10.1021/acsabm.1c01224

Singh, P., Vithalani, H., Adhyapak, A., Semwa, T., Singh, N., Dhanka, M.,…Saha, J. J. J. o. F. (2025). Microwave-assisted green synthesis of fluorescent graphene quantum dots: metal sensing, antioxidant properties, and biocompatibility insights. *Journal of Fluorescence*, 1-17. https://doi.org/https://doi.org/10.1007/s10895-025-04140-1

Su, J., Zhang, X., Tong, X., Wang, X., Yang, P., Yao, F.,…Yuan, C. J. M. L. (2020). Preparation of graphene quantum dots with high quantum yield by a facile one-step method and applications for cell imaging. *Materials Letters*, *271*, 127806. https://doi.org/https://doi.org/10.1016/j.matlet.2020.127806

Sun, H., Wu, L., Wei, W., & Qu, X. J. M. t. (2013). Recent advances in graphene quantum dots for sensing. *Materials Today*, *16*(11), 433-442. https://doi.org/https://doi.org/10.1016/j.mattod.2013.10.020

Surekha, G., Krishnaiah, K. V., Ravi, N., & Suvarna, R. P. (2020). FTIR, Raman and XRD analysis of graphene oxide films prepared by modified Hummers method. Journal of Physics: Conference Series, DOI 10.1088/1742-6596/1495/1/012012

Tian, R., Zhong, S., Wu, J., Jiang, W., Shen, Y., & Wang, T. J. O. M. (2016). Solvothermal method to prepare graphene quantum dots by hydrogen peroxide. *Optical Materials*, *60*, 204-208. https://doi.org/https://doi.org/10.1016/j.optmat.2016.07.032

Truong, K. T., Pham, T. H., & Van Tran, K. J. C. T. A. V. (2023). The impact of dimethylformamide on the synthesis of graphene quantum dots derived from graphene oxide. *Chimica Techno Acta*. https://doi.org/10.15826/chimtech.2023.10.4.05

Wang, L., Zhu, S.-J., Wang, H.-Y., Qu, S.-N., Zhang, Y.-L., Zhang, J.-H.,…Yang, B. J. A. n. (2014). Common origin of green luminescence in carbon nanodots and graphene quantum dots. *ACS Nano*, *8*(3), 2541-2547. https://doi.org/https://pubs.acs.org/doi/10.1021/nn500368m

Yan, H., He, C., Li, X., Zhao, T. J. D., & Materials, R. (2018). A solvent-free gaseous detonation approach for converting benzoic acid into graphene quantum dots within milliseconds. *Diamond and Related Materials*, *87*, 233-241. https://doi.org/https://doi.org/10.1016/j.diamond.2018.06.008

Yang, K., Feng, L., & Liu, Z. J. A. d. d. r. (2016). Stimuli responsive drug delivery systems based on nano-graphene for cancer therapy. *Advanced Drug Delivery Reviews*, *105*, 228-241. https://doi.org/https://doi.org/10.1016/j.addr.2016.05.015

Ye, Z., Lin, X., Wang, N., Zhou, J., Zhu, M., Qin, H., & Peng, X. J. N. C. (2021). Phonon-assisted up-conversion photoluminescence of quantum dots. *Nature Communications*, *12*(1), 4283. https://doi.org/https://doi.org/10.1038/s41467-021-24560-4

Yu, G. J., Yoo, J. H., Kwon, S. B., Yoo, H. C., Lee, U. Y., Kang, B. G.,…Interfaces. (2025). Green synthesis of nitrogen-doped graphene quantum dots by recycling waste graphite and impact of oxygen adsorption on enhancing photoluminescence. *Surfaces and Interfaces*, *64*, 106342. https://doi.org/doi:https://doi.org/10.1016/j.surfin.2025.106342

Yu, J., Liu, S., Chen, S., Wang, T. J. I., & Research, E. C. (2017). Simultaneous preparation of mesoporous/macroporous graphene aerogels and bright green photoluminescent graphene quantum dots by a simple solvothermal method. *Industrial & Engineering Chemistry Research*, *56*(36), 10028-10035. https://doi.org/https://pubs.acs.org/doi/10.1021/acs.iecr.7b01954

Zeng, G., Li, X.-X., Li, Y.-C., Chen, D.-B., Chen, Y.-C., Zhao, X.-F.,…Interfaces. (2022). A heterostructured graphene quantum dots/β-Ga2O3 solar-blind photodetector with enhanced photoresponsivity. *ACS Applied Materials & Interfaces*, *14*(14), 16846-16855. https://doi.org/https://pubs.acs.org/doi/10.1021/acsami.2c00671

Zhang, H., Guo, R., Li, S., Liu, C., Li, H., Zou, G.,…Ji, X. J. N. E. (2022). Graphene quantum dots enable dendrite-free zinc ion battery. *Nano Energy*, *92*, 106752. https://doi.org/https://doi.org/10.1016/j.nanoen.2021.106752

Zhang, J., Nan, D., Pan, S., Liu, H., Yang, H., Hu, X. J. S. A. P. A. M., & Spectroscopy, B. (2019). N, S co-doped carbon dots as a dual-functional fluorescent sensor for sensitive detection of baicalein and temperature. *Spectrochimica Acta Part A: Molecular and Biomolecular Spectroscopy*, *221*, 117161. https://doi.org/https://doi.org/10.1016/j.saa.2019.117161

Zhang, Z., Chang, K., Peeters, F. J. P. R. B. C. M., & Physics, M. (2008). Tuning of energy levels and optical properties of graphene quantum dots. *Physical Review B*, *77*(23), 235411. https://doi.org/DOI: https://doi.org/10.1103/PhysRevB.77.235411

Zheng, J., Xie, Y., Wei, Y., Yang, Y., Liu, X., Chen, Y., & Xu, B. J. N. (2020). An efficient synthesis and photoelectric properties of green carbon quantum dots with high fluorescent quantum yield. *Nanomaterials*, *10*(1), 82. https://doi.org/https://doi.org/https://doi.org/10.3390/nano10010082.

Zhu, S., Song, Y., Zhao, X., Shao, J., Zhang, J., & Yang, B. J. N. r. (2015). The photoluminescence mechanism in carbon dots (graphene quantum dots, carbon nanodots, and polymer dots): current state and future perspective. *Nano Research*, *8*, 355-381. https://doi.org/https://doi.org/10.1007/s12274-014-0644-3

Zhu, S., Zhang, J., Qiao, C., Tang, S., Li, Y., Yuan, W.,…Hu, R. J. C. c. (2011). Strongly green-photoluminescent graphene quantum dots for bioimaging applications. *Chemical Communications*, *47*(24), 6858-6860. https://doi.org/https://doi.org/10.1039/C1CC11122A

Zu, F., Yan, F., Bai, Z., Xu, J., Wang, Y., Huang, Y., & Zhou, X. J. M. A. (2017a). The quenching of the fluorescence of carbon dots: a review on mechanisms and applications. *Microchimica Acta*, *184*, 1899-1914. https://doi.org/https://doi.org/10.1007/s00604-017-2318-9

Zu, F., Yan, F., Bai, Z., Xu, J., Wang, Y., Huang, Y., & Zhou, X. J. M. A. (2017b). The quenching of the fluorescence of carbon dots: a review on mechanisms and applications. *Microchimica Acta*, *184*(7), 1899-1914. https://doi.org/DOI 10.1007/s00604-017-2318-9